AUTOMATED LABELING OF LOG FEATURES IN CT IMAGERY OF MULTIPLE HARDWOOD SPECIES

Daniel L. Schmoldt

USDA Forest Service
Biological Systems Engineering Department
460 Henry Mall
University of Wisconsin
Madison, WI 53706-1561

Jing He[1]

Communication Technology Group
COMSAT LAB
22300 COMSAT Drive
Clarksburg, MD 20871

and

A. Lynn Abbott

Associate Professor
Bradley Department of Electrical and Computer Engineering
Virginia Tech
Blacksburg, VA 24061-0111

(Received May 1999)

ABSTRACT

Before noninvasive scanning, e.g., computed tomography (CT), becomes feasible in industrial sawmill operations, we need a procedure that can automatically interpret scan information in order to provide the saw operator with information necessary to make proper sawing decisions. To this end, we have worked to develop an approach for automatic analysis of CT images of hardwood logs. Our current approach classifies each pixel individually using a feed-forward artifical neural network (ANN) and feature vectors that include a small, local neighborhood of pixels and the distance of the target pixel to the center of the log. Initially, this ANN was able to classify clear wood, bark, decay, knots, and voids in CT images of two species of oak with 95% pixel-wise accuracy. Recently we have investigated other ANN classifiers, comparing 2-D versus 3-D neighborhoods and species-dependent (single species) versus species-independent (multiple species) classifiers using oak (*Quercus rubra* L. and *Q. nigra* L.), yellow-poplar (*Liriodendron tulipifera* L.), and black cherry (*Prumus serotina* Ehrh.) CT images. When considered individually, the resulting species-dependent classifiers yield similar levels of accuracy (96–98%). 3-D neighborhoods work better for multiple-species classifiers, and 2-D is better for the single-species case. Classifiers combining yellow-poplar and cherry data misclassify many pixels belonging to splits as clear wood, resulting in lower classification rates. If yellow-poplar was not paired with cherry, however, we found no statistical difference in accuracy between the single- and multiple-species classifiers.

Keywords: Industrial inspection, segmentation, computed tomography, image analysis, log processing.

INTRODUCTION

Because the value of hardwood lumber is inversely proportional to the quantity and sizes of defects, log breakdown strategies generally seek to minimize defects in the resulting boards. Traditionally, the sawyer chooses an opening face by visually examining the exterior of a log and then dynamically adjusting the cutting face as sawing exposes the log interior. Sawing logs under different log orien-

[1] Formerly Graduate Research Assistant, Bradley Department of Electrical and Computer Engineering, Virginia Tech, Blacksburg VA 24061-0111.

Wood and Fiber Science, 32(3), 2000, pp. 287–300

tations and using different sawing methods greatly impact lumber value (Richards et al. 1980; Steele et al. 1994; Tsolakides 1969; Wagner et al. 1990, 1989). This type of sawing, however, is "information limited" in the sense that the sawyer has knowledge only of external indicators of internal features (e.g., defects) (Occeña et al. 1997). This greatly limits the sawyer's ability to achieve potential log value recovery. Developing nondestructive sensing and analysis methods that can accurately detect and characterize interior defects is critical to future efficiency improvements for sawmills (Occeña 1991).

A tacit assumption for eventual application of internal scanning to log sawing is that knowledge of internal defects will lead to greater sawyer productivity. Schmoldt (1996) identifies several operational scenarios: provide a 3-D image of the log as sawing occurs ("glass log") so that the sawyer can choose a best opening face using more complete (internal) log information, couple computer rendering of the log and its orientation on the carriage to accurately control log positioning by manipulating the computer rendition, have the computer suggest a best opening face to the sawyer and automatically position the log for that cut, or have the computer suggest the next face to cut during grade sawing by tying log face rendering to computerized lumber grading software. Log breakdown assisted by 3-D rendering is "fully informed," where the sawyer has knowledge about internal feature size, type, and location. CT scanning has been investigated as providing that internal feature information (Aune 1995; Benson-Cooper et al. 1982; Birkeland and Holoyen 1987; Burgess 1985; Cown and Clement 1983; Davis and Wells 1992; Grönlund 1992; Grundberg and Grönlund 1992; Harless et al. 1991; Hodges et al. 1990; Hopkins et al. 1982; Lindgren 1991; Onoe et al. 1984; Roder 1989; Schmoldt 1996; Taylor et al. 1984). However, because CT scanner design and development have focused on medical applications, an industrial CT scanner specifically designed for hardwood log processing does not exist (Schmoldt 1996). While we are actively pursuing industrial scanner development, we are also developing the necessary image interpretation software to automatically recognize internal log features and present this information to the sawyer in a useful manner.

Early work on automatically labeling internal log defects established the feasibility of utilizing CT images for this purpose. These researchers employed a variety of methods to segment different regions of a CT image and then to interpret, or label, those segmented regions. Often, image segmentation methods are based on threshold values derived from image histograms (Som et al. 1992; Taylor et al. 1984; Zhu et al. 1991c). Texture-based techniques have been applied only to defect labeling (Funt and Bryant 1987; Zhu et al. 1991b), and not to segmentation. Knowledge-based classification (Zhu et al. 1991a, 1996), shape examination (Funt and Bryant 1987; Som et al. 1992), and morphological operations (Som et al. 1992) have also been used to label defects.

While these efforts have demonstrated feasibility, they have some serious limitations. First, reports of defect labeling accuracy are often either anecdotal, based on success in a training set, or based on a single test set. No statistically valid estimates of labeling accuracy can be found in the literature. Second, there has been no effort to assess or to achieve real-time operability of the developed algorithms. Third, while texture information is intrinsic to human differentiation of regions in CT images (i.e., image segmentation), it has not been fully exploited in automated recognition algorithms.

Recent work by us (Li et al. 1996; Schmoldt et al. 1997) has demonstrated highly accurate labeling of log defects in CT imagery. In contrast to the previous global approaches that separate the tasks of segmentation and region labeling, this approach operates using local pixel neighborhoods primarily, and effectively combines segmentation and labeling into a

single classification step. A feed-forward artificial neural network (ANN) has been trained to accept CT values from a small 3-dimensional (3-D) neighborhood about the target pixel (using 3 adjacent CT images), and then to assign to each pixel a particular class label. In order to accommodate different types of hardwoods, a histogram-based preprocessing step normalizes CT density values prior to ANN classification. Morphological postprocessing is used to refine the shapes of detected image regions. This approach avoids the limitations of previous approaches, that is, accuracy can be evaluated quantitatively, defect labeling can be accomplished in real time, and texture information is utilized in the segmentation-classification step.

Accuracy achieved by this classification approach is very high (95%) at the pixel level (Schmoldt et al. 1997). This previous work, however, used two species of oak only (*Quercus rubra* L. and *Q. nigra* L.), and processed 3-D neighborhoods almost exclusively. The current study extends that work to additional species (yellow-poplar *Liriodendron tulipifera* L. and black cherry *Prumus serotina* Ehrh.) and examines the interaction of neighborhood dimensionally (2-D vs. 3-D) and single- vs. multiple-species classifiers, with respect to their impact on classifier accuracy. The issue that we sought to resolve here is whether we could develop a *species-independent* classifier of high accuracy that works well for several hardwood species simultaneously.

NEURAL NET CLASSIFIERS

We have developed species-dependent classifiers and species-independent classifiers for different local neighborhoods in CT images. Both 2-D and 3-D neighborhoods have been considered. All of these classifiers contain the same modules, which are: (1) a preprocessing module, (2) an ANN-based classifier, and (3) a postprocessing module—more details on these components can be found elsewhere (Li 1996; Li et al. 1997; Schmoldt et al. 1997). The preprocessing module separates wood from background and internal voids and normalizes the CT density values. The ANN classifier labels each pixel of the image as either clear wood or a particular type of defect. The postprocessing step removes some of the spurious misclassifications. The major difference between the various classifiers is that they are trained with different species' data and different types of input features, and therefore have different sets of ANN weights.

Classifiers

The ANN classifier is the seminal part of this log feature labeling system. Back-propagation neural networks were chosen because their documented effectiveness for pattern-matching problems, and their relative ease of use. Using an ANN, each nonbackground pixel is labeled. This section describes the procedure for generating a classifier, which includes extracting the input features for classification from the CT images and constructing the neural networks for 2-dimensional and 3-dimensional analysis.

Feature extraction.—Selecting useful features for an ANN is extremely important because they determine how well the classifier learns and consequently how it will perform in the future. In this work, the primary feature values that serve as input to the ANN are the histogram-normalized values of the pixels from a CT image. These pixels belong to the neighborhood of the pixel under consideration (the target pixel). For 2-D analysis, a pixel's neighborhood contains the pixels within a 5×5 window (Fig. 1a); for 3-D analysis, its neighborhood contains the pixels within a $3 \times 3 \times 3$ window, i.e. including 3×3 windows from adjacent CT images (Fig. 1b). Additionally, because some defects, such as splits, are near to the center, and some of them, such as bark and sapwood, are close to the outside edge of the log, the distance from the center of the log to the target pixel is also used as a feature value. This distance measure contains contextual (or global) information that can improve classification.

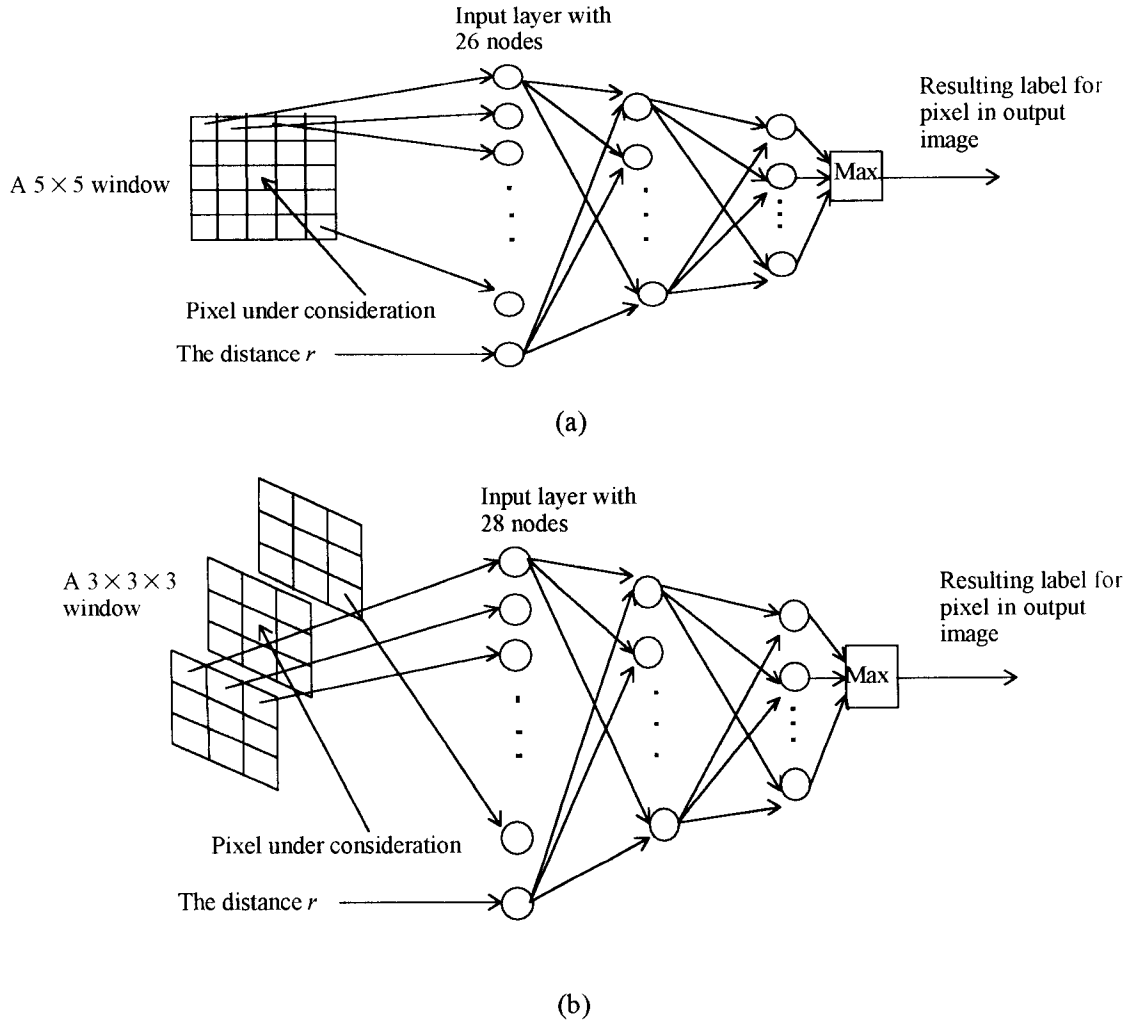

FIG. 1. ANNs containing a 2-D window (a) and a 3-D window (b) illustrate the network topology and relationship of input images to output classifications. The top left pixel in (a) is the input of the first node in the 2-D ANN, while the top left pixel in the previous slice (b) is mapped to the input for the first input node of the 3-D ANN. The radial distance r is the last input to the ANN in both cases.

To summarize, in order to label a particular pixel in a CT image, the feature vector that serves as input to the ANN for the 2-dimensional case contains the 25 normalized density values from the 5 × 5 neighborhood that is centered at the target pixel, plus the radial distance of the target pixel from the center of the log. For the 3-dimensional case, the feature vector contains the 27 normalized density values from the 3 × 3 × 3 neighborhood that is centered at the target pixel, plus the distance of the target pixel from the center of the log. Therefore, the total number of features for each target pixel in 2-D analysis is 26, and in 3-D analysis, the total number is 28.

Topology.—The topology of a neural network has an effect on the speed of convergence during training, and on the accuracy of the classification. Based on prior results (Li et al. 1996), we used a single hidden layer with 12 nodes. The numbers of output nodes for the ANNs differ, however. In different families of

TABLE 1. *Distribution of training/testing samples taken from different logs and different species. Decay was not present in the yellow-poplar samples, and sapwood was not distinguished in the other species. The labels "cherry_170" and "cherry_512" represent the same image data at different spatial resolutions.*

Species	Feature type					
	Clear wood	Knots	Bark	Splits	Decay	Sapwood
cherry_170	47%	16%	15%	11%	11%	
cherry_512	43%	16%	17%	12%	12%	
red oak	38%	13%	16%	17%	16%	
yellow-poplar	46%	15%	15%	5%		19%

species-dependent and species-independent classifiers, there are different defects to be labeled. For example, the red oak classifiers detect five classes: clear wood, knots, bark, splits, and decay; while the yellow-poplar/red oak combined classifiers identify six classes: heartwood/clear wood, knots, bark, splits, decay, and yellow-poplar sapwood. For all single-species classifiers, there are only five classes, and either five or six classes for the multiple-species classifiers. We have chosen important and common defects that occur in Eastern U.S. hardwoods—those being knots, decay, splits, bark, and other voids. Holes and large ring shake/splits are voids that the initial background preprocessing step will segregate from the wood and preclassify automatically. Stain is not a density-related defect (at least to any great extent), so CT values will be unaffected by their presence. Bark can occur internally (overgrown knots) or externally (scanning may occur prior to debarking). In our 2-D classifiers, the topology is therefore 26-12-5 or 26-12-6, which means that the structure of the neural network has 26 input nodes, 12 hidden nodes, and 5 or 6 output nodes. In 3-dimensional classifiers, the topology is 28-12-5 or 28-12-6, which has a similar interpretation.

Training and testing

An entire training/testing set for one hardwood species consists of approximately 1,000 samples. Ten-fold cross validation was used to evaluate the accuracy of each classifier. This means that the full training set is divided randomly into 10 mutually exclusive test partitions of approximately equal size. For each of the 10 stages of training, one partition is designated as the test set, and the remaining samples in the other partitions are used to train the neural network. In successive stages, different partitions are used for testing and the remaining samples are used for training. The average classification accuracy over all 10 stages of training is reported as the cross-validated classification accuracy.

In this work, all the ANNs were trained using the delta rule, which is a learning rule that specifies how connection weights are updated during the learning process. Momentum and learning rate parameters affect the operation of the learning rule. In particular, they affect the speed of convergence of the ANN weights. With a slow learning rate, the neural network converges very slowly. A momentum term is added to the delta rule to solve this problem. This momentum term accelerates learning by increasing weight changes when they are repeatedly in the same direction. Based on Li's results (Li et al. 1996), a small learning rate 0.1 and a medium momentum term 0.6 were selected as the learning parameters for all ANN training of hardwood log CT images. Random values were used as the initial weights for each network training session.

EXPERIMENTAL DESIGN

As noted above, 1,000 samples were taken from each of the species: red oak (including *Q. rubra and Q. nigra*), yellow-poplar, and black cherry. The percentages of these samples for each feature type across the different species appear in Table 1. Using these sam-

ples, we trained and tested several classifiers: the single-species classifiers are red oak (RO), yellow-poplar (YP), 170 × 170 cherry (CH), and 512 × 512 cherry (CH_512); the two-species classifiers are cherry/red oak (CH_RO), cherry/yellow-poplar (CH_YP), red oak/yellow-poplar (RO_YP); and the final cases have all 3 species combined (COMB).

Both red oak and yellow-poplar images have pixel resolution 2.5 × 2.5 × 2.5 mm^3. However, the cherry log images were generated by a different scanner at a different resolution, approximately 0.95 × 0.95 × 0.95 mm^3. Because image texture is noticeably different at these two resolutions, we did not combine data across resolutions for multiple-species classifier development. Instead, 3 × 3 × 3 neighborhoods in the 512 × 512 cherry images (cherry_512) were averaged to produce new images (cherry_170) with approximately 2.84 × 2.84 × 2.84 mm^3 resolution. We concluded that these resampled images would provide comparable texture to our earlier 2.5 × 2.5 × 2.5 mm^3 images. Having multiple resolutions within the same species also allowed us to compare classifier accuracy for two different image resolutions.

Initial attempts to process yellow-poplar images used a 28-12-4 topology for the 3-D ANN, which means that this preliminary classifier had four outputs: clear wood, knots, bark, and splits (decay is not present in our yellow-poplar images). For yellow-poplar logs in which both heartwood and sapwood are present, the classifier performed quite poorly (Fig. 2b). This occurred because CT image values (density) for heartwood and sapwood are very different in yellow-poplar. This is visually apparent in Fig. 2a. Therefore, it was necessary to distinguish yellow-poplar sapwood from the generalized clear wood class (adding an additional classifier output for this class) in order to develop accurate classifiers that used yellow-poplar image data (Li et al. 1997). Figure 2c illustrates that when sapwood is included as a distinct label from clear wood, sapwood mislabelings disappear. Subsequent application of labeled information can then merge yellow-poplar heartwood and sapwood into a single *clear wood* class. Extremely low-density regions (also, long and thin) in the heartwood near the center of the log (the typical location for splits) are misclassified as splits, however. To eliminate these errors, additional training samples can be added to the data set from these error-prone regions, and a new classifier can be trained (Fig. 2d).

Using ten-fold cross-validation, we developed individual classifiers for each species—red oak, yellow-poplar, and cherry—using both 2-D and 3-D feature vectors (six classifiers). Images used were the nominal $(2.5\text{-mm})^3$ resolution. We also developed multiple-species classifiers: pairing two species at a time and combining all three species together. These were also trained using 2-D and 3-D feature vectors for a total of eight multiple-species classifiers. Finally, the finer resolution cherry images $(0.95\text{ mm})^3$ were used to train both a 2-D and 3-D classifier.

RESULTS AND DISCUSSION

Classification accuracies for the different classifiers appear in Fig. 3. These line plots seem to indicate that the 2-D approach has higher accuracy than 3-D for single-species classifiers; the reverse appears to be true for multiple-species classifiers. This result can be verified visually in Fig. 4, where two oak images are labeled using both 2-D and 3-D classifiers in which the former appears to perform better. However, it is impossible to determine from these performance estimates (Fig. 3) whether these apparent differences in accuracy reflect real differences. Because ten-fold cross-validation was used, each trained classifier actually has 10 estimates of classification accuracy, resulting from the accuracy rates from each partition of the training/testing sets (Fig. 5). Therefore, these estimates can be used as samples in statistical Analysis of Variance (ANOVA).

In our first statistical test, we separate the full set of classification rates into two groups: *dimensionality*, which includes two-dimen-

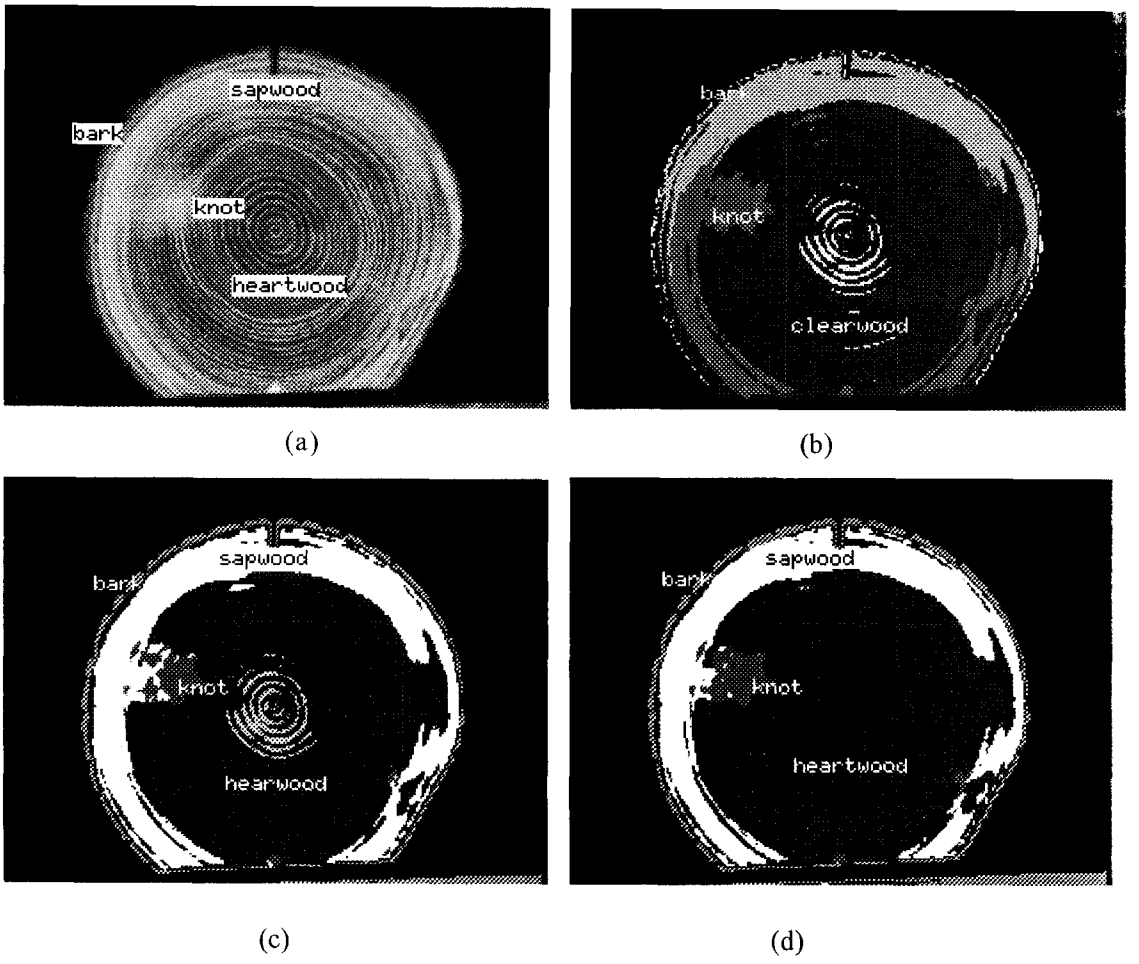

FIG. 2. A CT image (256 × 256) from a yellow-poplar log with knots, bark, sapwood, and heartwood labeled illustrates the density value difference between heartwood and sapwood (a). When this image (a) is labeled using a 3-D classifier with only four outputs (no separate sapwood class), sapwood regions are mislabeled as bark (b). A second 3-D classifier (including a sapwood class) applied to the same image (a) results in visually more accurate labeling (c), with the exception of annual rings mislabeled as splits. This latter classifier, trained with additional samples from the error-prone section of yellow-poplar logs, now correctly ignores annual rings and treats them as belonging to clear wood (d).

sional and three-dimensional classifiers, and *cardinality*, which includes single (species-dependent) and multiple (species-independent) classifiers. ANOVA treatments, in this case, are single and multiple cardinality, and are blocked on the dimensionality of the classifiers (2-D or 3-D) because we wish to test the hypothesis that there is no difference in accuracy for species-dependent and species-independent classifiers. The F-ratio results for the dimensionality and cardinality are 0.055 ($P = 0.815$) and 27.4 ($P < 0.001$), respectively. It is clear that the F ratio for cardinality indicates (at this point) that significant differences exist between the mean classification rates for the single- and multiple-species classifiers.

The interaction of dimensionality and cardinality is also significant ($P = 0.018$), indicating a combined effect. This can be seen in the average classification rates of Fig. 3, where 2-D rates are generally higher for single-species classifiers and 3-D rates are generally

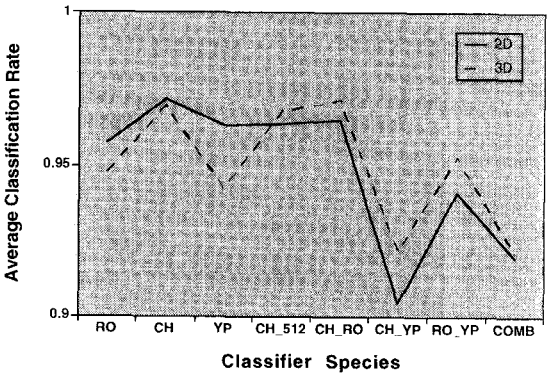

FIG. 3. 2-D and 3-D classifier accuracies are plotted for each of the ANN classifiers—red oak (RO), cherry (CH), yellow-poplar (YP), 512 × 512 cherry (CH_512), cherry/red oak (CH_RO), cherry/yellow-poplar (CH_YP), red oak/yellow-poplar (RO_YP), and all 3 species combined (COMB).

higher for multiple-species classifiers. To determine which means are significantly different for cardinality and dimensionality, post-hoc pairwise *t*-tests were performed. The probability values associated with those tests are shown in Table 2. The important thing to notice about this table is that while 2-D multiple-species classifiers have significantly different classification rates from 2-D single-species classifiers (cardinality differences), 3-D multiple-species classifiers are not significantly different from 3-D single-species classifiers (i.e., no cardinality differences). This results from the overall middle-ground rates of the 3-D classifiers. As visual examples of this, the CT image in Fig. 2a is labeled by a 3-D RO_YP classifier (Fig. 6a) and a 3-D COMB classifier (Fig. 6b). Both appear to match the 3-D single-species classifier image of Fig. 2d quite closely.

To understand greater details about the differences between dimensionality and cardinality, we performed ANOVAs for single- and multiple-species classifiers separately. For the single-species classifiers, ANOVA treatments are species (CH, RO, and YP), and dimensionality (2-D and 3-D) is used for blocking. F-ratio values for species and dimensionality are 11.4 ($P < 0.005$) and 9.53 ($P = 0.003$), respectively. Probability values associated with post-hoc *t*-tests demonstrate that the classification rates for the cherry-specific classifier is significantly different from both those of the red oak- and the yellow-poplar-specific classifiers. However, there is no significant difference between the red oak and yellow-poplar single-species classifiers.

For the multiple-species classifiers, ANOVA treatments are species (CH_RO, CH_YP, COMB, RO_YP), and dimensionality (2-D and 3-D) is used for blocking. F-ratio values for species and dimensionality are 39.3 ($P < 0.005$) and 4.97 ($P = 0.032$), respectively. Probability values associated with post-hoc *t*-tests indicate that the CH_RO classifier has significantly greater accuracy than the other three multiple-species classifiers. In addition, the RO_YP classifier has greater accuracy than the two lowest-accuracy classifiers, COMB and CH_YP. Both of those latter two classifiers contain both cherry and yellow-poplar samples, which apparently create classification problems. *T*-tests indicate that COMB and CH_YP are not significantly different from one another.

Based on the obvious classification problems stemming from combining cherry and yellow-poplar samples, we performed our original ANOVA again. This time, treatments were cardinality again, but only CH_RO and RO_YP were included in the multiple-species classifiers (no cherry/yellow-poplar combina-

→

FIG. 4. Two examples of CT images of red oak logs processed by 2-D and 3-D classifiers: (a) an original CT image; (b) a second CT image; (c) the result of image (a) labeled by the 2-D oak classifier; (d) the result of image (b) labeled by the same 2-D classifier; (e) the result of image (a) labeled by the 3-D oak classifier; (f) the result of image (b) labeled by the same 3-D classifier. (Images (e) and (f) were generated by Li (1996) and used a different postprocessing method.)

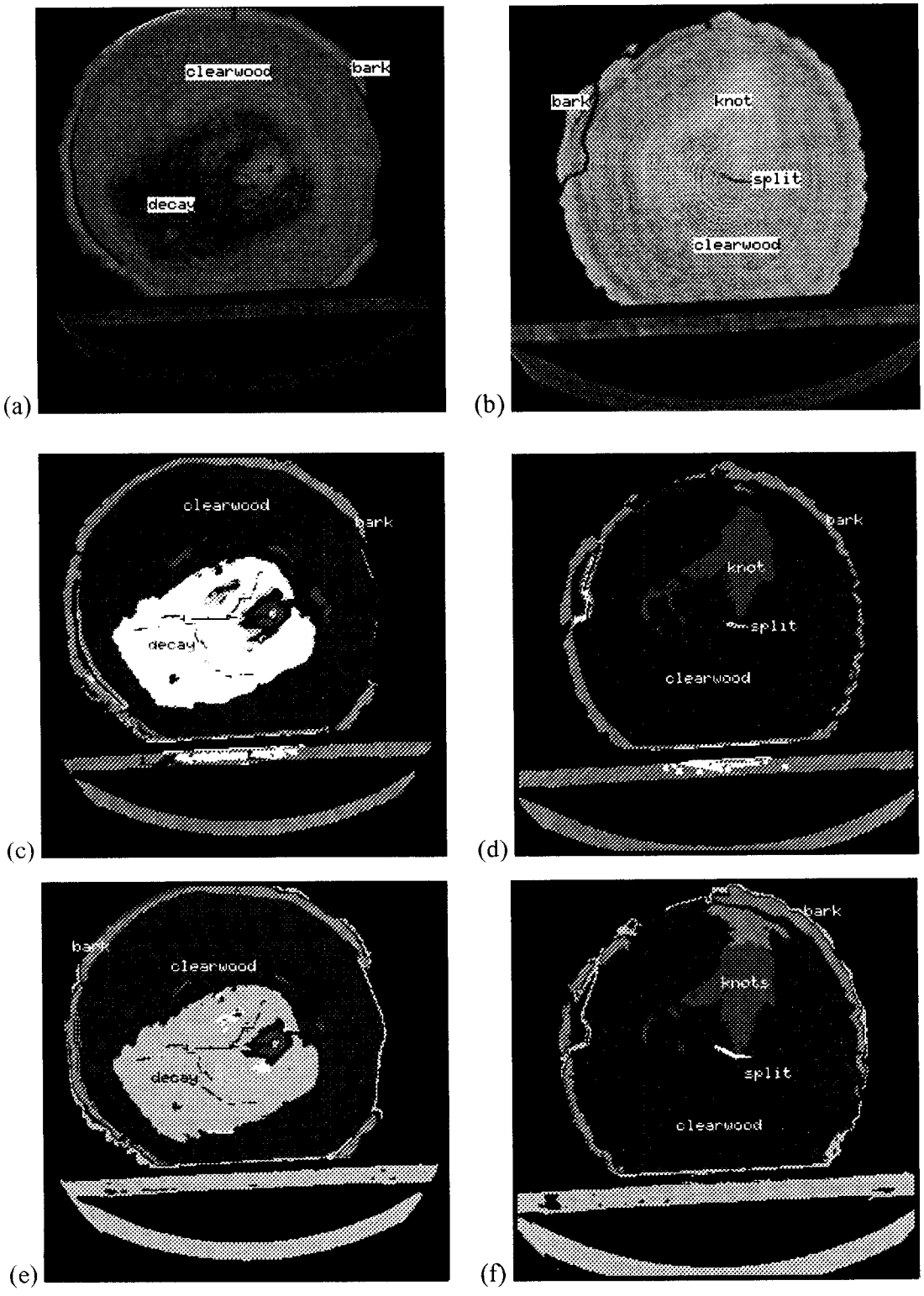
clearwood
bark
decay
(a)
bark
knot
split
clearwood
(b)
clearwood
bark
decay
(c)
bark
knot
split
clearwood
(d)
bark
clearwood
decay
(e)
bark
knots
split
clearwood
(f)

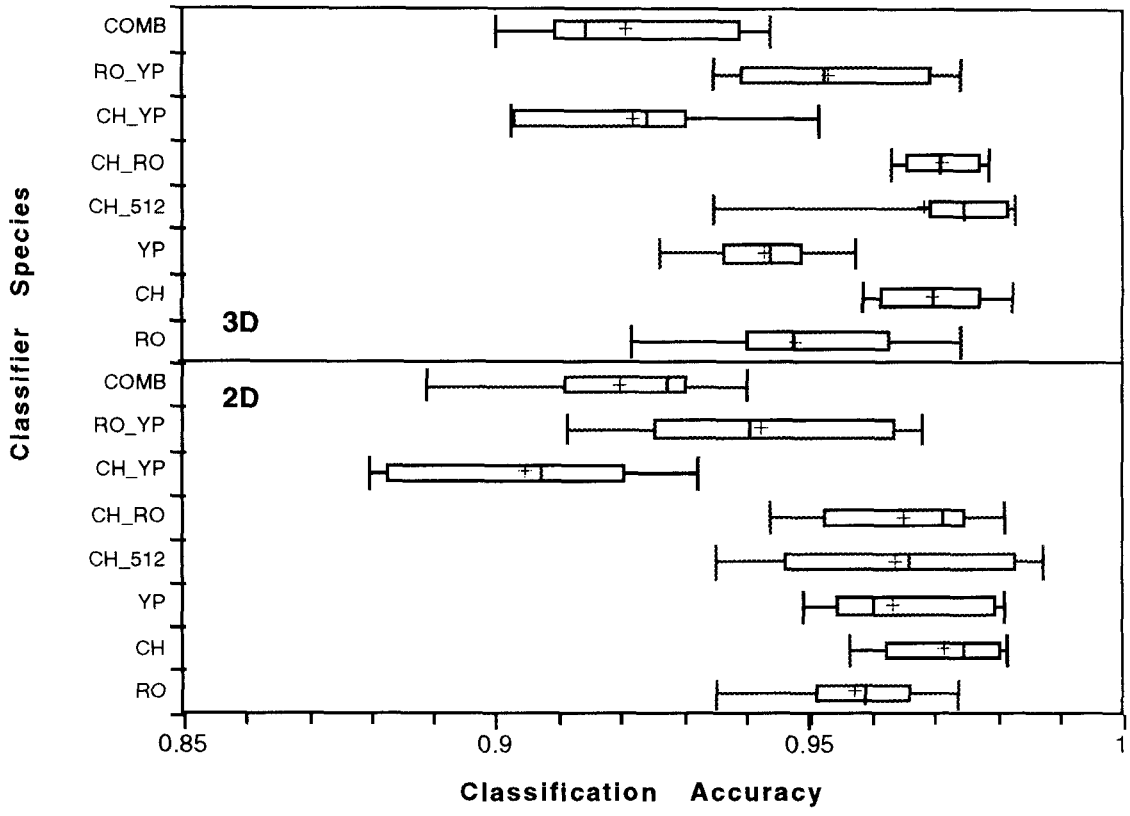

FIG. 5. A box plot of the classification rates provides more information that the graph of average values. The box ends are 25th and 75th percentile ranges, respectively. The whiskers represent the 10th and 90th percentiles, respectively. The line within the box is the median, and the cross is the mean.

tions). Also, the fine resolution (0.95-mm) cherry classifier (CH_512) was excluded from the single-species classifiers. As before, we blocked the ANOVA on dimensionality (2-D and 3-D). The resulting F-ratio value for cardinality is 0.050, which indicates that there is no real difference between single- and multiple-species classification rates when cherry/yellow-poplar combinations are excluded.

Finally, we performed an ANOVA to compare the effect of CT resolution on classifier performance. We eliminated the effect of dimensionality by blocking on it, as before, and found that the finer resolution cherry classifier has no significantly different classification rate than the coarser resolution cherry classifier in our study.

As illustrated above and Fig. 2d, it is possible to improve labeling accuracy by increasing the number of samples from those regions that currently produce errors. These improvements can result, however, in increased errors elsewhere. For example, the confusion matrix for the 3-D all-species classifier (Table 3)

TABLE 2. *A matrix of pair-wise t-test probability values for different classification rates for various combinations of dimensionality and cardinality. "2-D" and "3-D" refer to the spatial extent of the pixel neighborhoods used in classification. "Single" and "multiple" refer to the number of species considered by the classifier.*

	2-D multiple	2-D single	3-D multiple	3-D single
2-D multiple	1.000			
2-D single	0.000	1.000		
3-D multiple	0.347	0.001	1.000	
3-D single	0.002	0.301	0.187	1.000

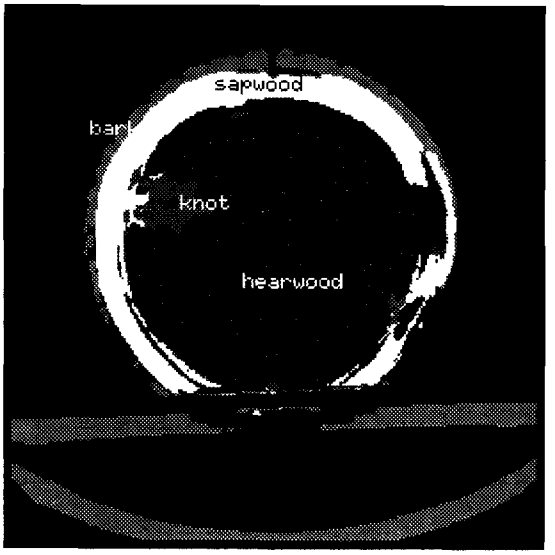

(a)

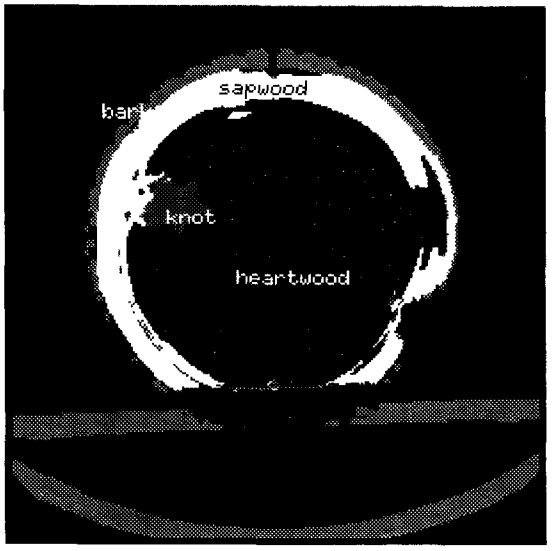

(b)

FIG. 6. The CT image of Fig. 2a is labeled by a 3-D multiple-species classifier (RO_YP) in (a) and the all-species classifier (COMB) in (b).

shows that many pixels that are actually contained in splits are now labeled as clear wood. This occurs because the added training samples are biased against splits and toward clear wood labeling, and few training samples for yellow-poplar and cherry splits are available (Table 1). This bias does not appear to affect the confusion matrices for the two, yellow-poplar classifiers, but is the primary source of error whenever yellow-poplar is paired with oak or cherry in a classifier. The second most notable source of classification error is labeling clear wood pixels as bark. Due to the higher classification accuracies of the single-species classifiers, there are few significant trends apparent in their confusion matrices.

TABLE 3. *A confusion matrix for the 3D all-species classifier indicates where labeling errors occur (the off-diagonal elements).*

	Actual class					
Classified as:	Clear wood	Knot	Bark	Split	Decay	Sapwood
Clear wood	1,266	16	36	85	23	1
Knot	3	389	0	0	2	2
Bark	45	7	425	0	0	3
Split	11	0	0	226	10	0
Decay	8	0	2	7	236	0
Sapwood	0	32	15	0	0	226
Total	1,333	444	478	318	271	232

CONCLUSIONS

Six single-species classifiers (ignoring the higher-resolution case for cherry) were trained using both 2-D and 3-D image data. The accuracy of all six classifiers is above 95%. Six, two-species classifiers have also been trained using both 2-D and 3-D image data. Two of them are red oak and yellow-poplar combined classifiers, two of them are red oak and cherry combined classifiers, and two are cherry and yellow-poplar combined classifiers. Their accuracy is 90%–97%. Finally, combined three-species classifiers (red oak, yellow-poplar, and cherry) were generated for 2-D and 3-D analysis. These two classifiers identified six kinds of defects: clear wood, knot, bark, split, decay, and yellow-poplar sapwood. Their accuracy is about 91%–92%.

Even at the lowest accuracies, all defects are identified in all images. However, because our classifiers operate on a pixel-by-pixel basis, the extent of those defects is not always de-

scribed entirely. In addition, small areas of pixels with false labelings remain following postprocessing. Our current morphological operations do not eliminate them entirely. Furthermore, the resulting classified image is a raster of individual pixels rather than a set of connected regions. Two primary avenues for improvement of this approach are to expand the postprocessing step to include region growing and to apply intelligent postprocessing of those regions to eliminate false labelings.

In comparing 2-D and 3-D features, the performance of 2-D single-species classifiers is better than that of 3-D classifiers. The performance of 3-D multiple-species classifiers is better than that of 2-D classifiers. We conjecture that in single-species classification multiple image planes contain redundant data that may be unimportant, or even counterproductive, for accurate classification. For multiple-species classification, however, the extra information contained in previous and subsequent CT slices seems to aid feature labeling. Consequently, as we increase the species mix that a classifier must accommodate, it appears that 3-D features are important for attaining high accuracy.

Higher-resolution images do not seem to have a significant difference on classifier performance. We were able to achieve similar accuracies in cherry using ~1 mm spatial resolution and ~3 mm resolution. That is, if we can distinguish features visually (at whatever image resolution we happen to choose), then our classification approach can also distinguish those features automatically. Therefore, the match between visual and automated classification is the same regardless of resolution; the match between either of those classifications and physical reality is related, of course, to image quality (resolution). This implies that our ANN classification approach is general enough to be applied broadly to CT images of varying resolutions. All that is required is resolution-specific training so that the classifier can incorporate local texture information.

In comparing single-species classifiers and multiple-species classifiers, the performance of the former is better than that of the latter when cherry/yellow-poplar combinations are used. On the other hand, when those combinations are excluded, there is no significant difference between classification accuracy for single- and multiple-species classifiers. Yellow-poplar has traditionally been difficult to deal with because it possesses many intrinsic differences (wood structure, density) from most other fine-grained hardwoods, e.g., cherry. Yellow-poplar was included in the study because it is an extreme case, and we desired to delineate a worst-case scenario. Consequently, the difficulty we experienced in combining it with cherry here is neither surprising, nor particularly worrisome.

The primary reason for lower accuracies when combining yellow-poplar and cherry is that there are few split examples for either species in our data set. Combining that with the clear wood bias (vis-à-vis splits) in yellow-poplar samples noted previously, it is not surprising that the multiple-species classifiers were unable to separate the split class effectively. By obtaining more split samples from both species, we should be able to improve the performance of their combined classifiers.

All of these accuracies (90%–98%) should be acceptable for industrial use. Furthermore, it should be noted that all reported accuracies are *prior* to postprocessing. We have visually determined (via classified images) that postprocessing does improve accuracy, but we do not have a quantitative estimate for that improvement. Consequently, we expect that the range of accuracies after postprocessing is actually higher than reported above, which further enhances its applicability to industrial use.

REFERENCES

AUNE, J. 1995. The development of a log scanner for sawmills in Canada. *In* O. Lindgren, ed. 2nd International Seminar on Scanning Technology and Image Processing on Wood. Dept. of Wood Technology, Luleå University, Skellefteå, Sweden.

BENSON-COOPER, D. M., R. L. KNOWLES, F. J. THOMPSON, AND D. J. COWN. 1982. Computed tomographic scanning for the detection of defects within logs. Bull. No.

8 Forest Research Institute, New Zealand Forest Service, Rotorua, NZ. 9 pp.

BIRKELAND, R., AND S. HOLOYEN. 1987. Industrial methods for internal scanning of log defects: A progress report on an ongoing project in Norway. *In* R. Szymani, ed. 2nd International Conference on Scanning Technology in Sawmilling, 1–2 October, Oakland/Berkeley Hills, CA. Forest Industries/World Wood, San Francisco, CA.

BURGESS, A. E. 1985. Potential applications of medical imaging techniques to wood products. *In* R. Szymani, ed. 1st International Conference on Scanning Technology in Sawmilling, October 10–12, San Francisco, CA. Forest Industries/World Wood, San Francisco, CA.

COWN, D. J., AND B. C. CLEMENT. 1983. A wood densitometer using direct scanning with x-rays. Wood Sci. Technol. 17(2):91–99.

DAVIS, J. R., AND P. WELLS. 1992. Computed tomography measurements on wood. Ind. Metrology 2(3/4):195–218.

FUNT, B. V., AND E. C. BRYANT. 1987. Detection of internal log defects by automatic interpretation of computer tomography images. Forest Prod. J. 37(1):56–62.

GRÖNLUND, A. 1992. Benefits from knowing the interior of the log. *In* O. Lindgren, ed. 1st International Seminar on Scanning Technology and Image Processing on Wood, August 30–September 1, Skellefteå, Sweden. Dept. of Wood Technology, Luleå University, Skellefteå Sweden. 7 pp.

GRUNDBERG, S., AND A. GRÖNLUND. 1992. Log scanning—Extraction of knot geometry. *In* O. Lindgren, ed. 1st International Seminar on Scanning Technology and Image Processing on Wood, August 30–September 1, Skellefteå, Sweden. Dept. of Wood Technology, Luleå University, Skellefteå, Sweden. 11 pp.

HARLESS, T. E. G., F. G. WAGNER, P. H. STEELE, F. W. TAYLOR, V. YADAMA, AND C. W. MCMILLIN. 1991. Methodology for locating defects within hardwood logs and determining their impact on lumber-value yield. Forest Prod J. 41(4):25–30.

HODGES, D. G., W. C. ANDERSON, AND C. W. MCMILLIN. 1990. The economic potential of CT scanners for hardwood sawmills. Forest Prod. J. 40(3):65–69.

HOPKINS, F., I. L. MORGAN, H. ELLINGER, AND R. KLINKSIEK. 1982. Tomographic image analysis. Mater. Eval. 40(20):1226–1228.

LI, P. 1996. Automatic interpretation of computer tomography (CT) images for hardwood log defect detection. MS thesis, Virginia Tech, Blacksburg, VA.

———, A. L. ABBOTT, AND D. L. SCHMOLDT. 1996. Automated analysis of CT images for the inspection of hardwood logs. *In* Proc. 1996 IEEE International Conference on Neural Networks. Institute for Electrical and Electronics Engineers, Inc., Piscataway, NJ.

———, J. HE, A. L. ABBOTT, AND D. L. SCHMOLDT. 1997. Labeling defects in CT images of hardwood logs with species-dependent and species-independent classifiers. Pages 113–126 *in* A. Prinz and W. Pölzleitner, eds. Proc. International Association of Pattern Recognition Workshop on Machine Perception Applications, 2–3 September 1996, Technical University Graz, Austria. R. Oldenbourg, Vienna, Austria.

LINDGREN, L. O. 1991. Medical CAT-scanning: X-ray absorption coefficients, CT-numbers and their relation to wood density. Wood Sci. Technol. 25:341–349.

OCCEÑA, L. G. 1991. Computer integrated manufacturing issues related to the hardwood log sawmill. J. Forest Eng. 3(1):39–45.

———, D. L. SCHMOLDT, AND S. THAWORNWONG. 1997. Using internal defect information for log breakdown. Pages 63–68 *in* J. Dennig, ed. ScanPro: Advanced technology for sawmilling. Miller-Freeman, San Francisco, CA.

ONOE, M., J. W. TSAO, H. YAMADA, H. NAKAMURA, J. KOGURA, H. KAWAMURA, AND M. YOSHIMATSU. 1984. Computed tomography for measuring the annual rings of a live tree. Nuclear Instr. Methods Physics Res. 221(1): 213–220.

RICHARDS, D. B., W. K. ADKINS, H. HALLOCK, AND E. H. BULGRIN. 1980. Lumber value from computerized simulation of hardwood log sawing. Res. Pap. FPL-356. USDA, Forest Service, Forest Products Lab, Madison WI, 10 pp.

RODER, F. 1989. High speed CT scanning of logs. *In* R. Szymani, ed. 3rd International Conference on Scanning Technology in Sawmilling, October 5–6, San Francisco, CA. Forest Industries/World Wood, San Francisco, CA.

SCHMOLDT, D. L. 1996. CT imaging, data reduction, and visualization of hardwood logs. *In* D. Meyer, ed. Proc. 1996 Hardwood Research Symposium. National Hardwood Lumber Association, Memphis, TN.

———, P. LI, AND A. L. ABBOTT. 1997. Machine vision using artificial neural networks and 3D pixel neighborhoods. Computers and Electronics in Agriculture 16(3): 255–271.

SOM, S., P. WELLS, AND J. DAVIS. 1992. Automated feature extraction of wood from tomographic images. *In* Second International Conference on Automation, Robotics and Computer Vision, September 15–18, Singapore. 5 pp.

STEELE, P. H., T. E. G. HARLESS, F. G. WAGNER, L. KUMAR, AND F. W. TAYLOR. 1994. Increased lumber value from optimum orientation of internal defects with respect to sawing pattern in hardwood sawlogs. Forest Prod. J. 44(3):69–72.

TAYLOR, F. W., J. F. G. WAGNER, C. W. MCMILLIN, I. L. MORGAN, AND F. F. HOPKINS. 1984. Locating knots by industrial tomography—A feasibility study. Forest Prod. J. 34(5):42–46.

TSOLAKIDES, J. A. 1969. A simulation model for log yield study. Forest Prod. J. 19(7):21–26.

WAGNER, F. G., F. W. TAYLOR, P. H. STEELE, AND T. E. G. HARLESS. 1989. Benefits of internal log scanning. *In* R. Szymani, ed. 3rd International Conference on Scanning Technology in Sawmilling, October 5–6, San Francisco,

CA. Forest Industries/World Wood, San Francisco, CA. 7 pp.

———, T. E. G. HARLESS, P. H. STEELE, F. W. TAYLOR, V. YADAMA, AND C. W. MCMILLIN. 1990. Potential benefits of internal-log scanning. Pages 77–88 *in* Proc. Process Control/Production Management of Wood Products: Technology for the 90's, October 30–November 1, Athens GA. The University of Georgia, Athens, GA.

ZHU, D., R. W. CONNERS, F. M. LAMB, D. L. SCHMOLDT, AND P. A. ARAMAN. 1991a. A computer vision system for locating and identifying internal log defects using CT imagery. *In* R. Szymani, ed. 4th International Conference of Scanning Technology in Sawmilling, Oct. 28–31, San Francisco, CA. Forest Industries/World Wood, San Francisco, CA. 13 pp.

———, ———, L. SCHMOLDT, AND P. A. ARAMAN. 1991b. CT image sequence analysis for object recognition—A rule-based 3-d computer vision system. Pages 173–178 *in* 1991 IEEE International Conference on Systems, Man, and Cybernetics, October 13–16, Charlottesville, VA.

———, ———, AND P. A. ARAMAN. 1991c. CT image scquence processing for wood defect recognition. *in* Proc 23rd Southeast Symposium on System Theory, March, Columbia, SC. 7 pp.

———, ———, D. L. SCHMOLDT, AND P. A. ARAMAN. 1996. A prototype vision system for analyzing CT imagery of hardwood logs. IEEE Transactions on Systems, Man, and Cybernetics 26(4):522–532.